Green Synthesis of CuO-TiO_2-ZnO (CuTiZn) Ternary Nanocomposite via Kenger Gum Extract: A Study of their Structure, Characterization, and Biological Applications

Saniye Tekerek [a,*]

a. Department of Materials Science and Engineering, Graduate School of Natural and Applied Sciences, Kahramanmaraş Sutcu Imam University, Kahramanmaraş, Turkey-46100
https://orcid.org/0000-0003-3326-358X

*Corresponding author: saniyetekerek@ksu.edu.tr (S. Tekerek)

Accepted by Scientia Iranica

Abstract

This study presents the synthesis of CuO-TiO_2-ZnO (CuTiZn) ternary nanocomposite via the use of Kenger (Gundelia tournefortii) gum extract as a biogenic reducing and stabilizing agent. The synthesized CuTiZn nanocomposite was characterized via X-ray diffraction (XRD), scanning electron microscopy (SEM), and Fourier transform infrared spectroscopy (FTIR). XRD analysis confirmed the formation of a CuO-TiO_2-ZnO nanocomposite with a monoclinic crystal structure. SEM images revealed spherical, well-dispersed particles, whereas FTIR spectra indicated the presence of functional groups from the Kenger gum extract involved in the reduction process. Biological applications, including antibacterial activity against both gram-positive and gram-negative bacteria, were evaluated, yielding promising results. The antimicrobial activity of the biosynthesized ternary nanocomposite was evidenced by the formation of inhibition zones ranging from 13.5 to 18 mm in diameter against both gram-positive and gram-negative bacteria. The antioxidant properties were assessed via DPPH radical scavenging assays, which revealed an inhibition rate of approximately 34% at a concentration of 12.5 mg/mL. In anticancer activity assays, the CuTiZn nanocomposite exhibited an IC_{50} value of 201.1 µg/mL against the MCF-7 human breast cancer cell line. These findings suggest that the biosynthesized CuTiZn nanocomposite possesses promising antimicrobial, antioxidant, and anticancer properties, highlighting their potential for biomedical applications. This study, for the first time, uses the green synthesis of CuTiZn ternary nanocomposite using Kenger (Gundelia tournefortii) gum agent. This eco-friendly approach not only minimizes toxic reagents but also enables the production of multifunctional nanocomposite with superior antibacterial and cytotoxic performance due to the synergistic effects of the three metal oxides.

Keywords Nanocomposite; Antibacterial; Antioxidant; Cytotoxicity

Highlights

- Green synthesis of CuO-TiO_2-ZnO nanocomposites using *Kenger* (Gundelia) gum extract.
- Structural and morphological characterization confirmed ternary metal oxide formation.
- Nanocomposites showed enhanced antibacterial and antioxidant properties.
- Eco-friendly method promotes sustainable nanomaterial production.
- Synergistic effects among CuO, TiO_2, and ZnO boost biological performance.

1. Introduction

In recent years, the development of multifunctional nanomaterials with biomedical potential has gained significant attention. Among them, metal-based nanocomposite synthesized via green or biological routes have emerged as promising candidates because of their enhanced biocompatibility and functional properties. Nanocomposites have attracted considerable attention in recent years because of their unique properties, such as enhanced mechanical, electrical, and optical characteristics. These attributes make them suitable for a wide range of applications, especially in biomedical fields. Among various metal-based nanocomposite, CuO-TiO_2-ZnO (CuTiZn) combinations are of particular interest because of their synergistic effects, which enhance their antimicrobial and

anticancer properties. Traditionally, the synthesis of such nanocomposite has been carried out through chemical methods; however, with increasing environmental concerns, there is a growing demand for more sustainable approaches. Green synthesis, which involves the use of natural substances, offers an eco-friendly, cost-effective alternative to traditional methods.

The green synthesis of nanoparticles, which employs plant components enriched with diverse bioactive phytochemicals, provides significant advantages over conventional physical and chemical synthesis routes. These include environmental sustainability, the absence of contamination, faster processing, cost-effectiveness, and, most notably, the use of nontoxic and biocompatible natural agents for reducing and stabilizing nanoparticles [1]. In addition to its economic benefits and scalability, this approach eliminates the need for high pressure, electricity, elevated temperatures, and harmful chemicals, thereby improving both safety and sustainability [2]. The main applications of green synthesis for nanoparticles have been explored in areas such as antimicrobial catalysis, biomedical diagnostics, molecular sensing, biological system labeling, and optical imaging [3].

The increasing prevalence of antibiotic resistance and the limited effectiveness of conventional cancer treatments have highlighted the urgent need for novel therapeutic agents that offer improved efficacy and fewer side effects. In this context, nanomaterials have gained significant attention because of their promising potential in a wide range of biomedical applications, particularly in antimicrobial and anticancer therapies. Among the various types of nanocomposite, those synthesized via natural and eco-friendly methods have become particularly appealing because of their biocompatibility, sustainability, and minimal environmental impact. One such promising biotemplate is kenger gum, a natural polysaccharide obtained from kenger plants (*Gundelia tournefortii*), which has shown considerable potential in the synthesis of metal-based nanocomposite.

A key advantage of using kenger gum in nanocomposite synthesis is the adoption of a green synthesis approach. This eco-friendly method uses natural polysaccharides as reducing and stabilizing agents, eliminating the need for toxic chemicals commonly used in traditional chemical synthesis methods. The green synthesis approach not only ensures environmental sustainability but also enhances the biocompatibility of the resulting nanomaterials. This method has been successfully applied to the synthesis of various metal-based nanocomposite, including Cu, Ti, and Zn nanoparticles, which have a wide range of applications in antimicrobial, anticancer, and drug delivery systems.

Recent studies have highlighted the potential of green-synthesized ternary metal oxide nanocomposite for diverse environmental and biological applications. Existing studies in the literature have extensively examined the photocatalytic and antibacterial properties of ternary ZnO:NiO:CuO nanocomposite synthesized via a hydrothermal method under sunlight irradiation. These studies have shown enhanced photocatalytic performance, which is attributed to the synergistic effects among CuO, NiO, and ZnO. In addition to their photocatalytic activity, several studies have highlighted the antibacterial effects of these nanocomposite [4]. The antibacterial properties of TiO_2/ZnO composites, which effectively inhibit bacterial growth under UV light, have been reported. Similarly, CuO/TiO_2/ZnO nanocomposite exhibited significant antibacterial activity against both gram-positive and gram-negative bacteria, underscoring the multifunctional potential of these materials. The incorporation of CuO was shown to enhance the antibacterial effects, positioning these nanocomposite as promising candidates for environmental and health-related applications. Similarly, optimization of structural parameters, including grain size, surface area, and coating layers in TiO_2 thin films, has been shown to improve chemical oxygen demand (COD) removal efficiency under UVA irradiation [5]. Furthermore, hybrid systems, such as activated carbon/TiO_2 and AC/TiO_2/ZnO composites, enhance dye degradation and antibacterial performance, particularly when combined with micro-nano bubble aeration [5,6]. Similarly, MoS_2/SnS_2@AC nanocomposite maintain structural stability while efficiently degrading dyes under visible light and displaying dose-dependent antibacterial activity [7]. Notably, previous studies have shown that kenger gum itself exhibits significant antibacterial activity against Streptococcus mutans and salivary mutans streptococci, while exerting only moderate cytotoxic effects on non-tumorigenic fibroblast cells, highlighting its potential as a safe oral antimicrobial agent [8]. Collectively, these findings emphasize that integrating green synthesis, hybridization strategies, and structural optimization is crucial for the development of multifunctional nanocomposite with promising environmental and biomedical applications.

Gundelia tournefortii L., commonly known as kenger, is a medicinal plant native to the temperate regions of Western Asia, including Turkey, Iran, and Iraq [9]. It is rich in bioactive compounds, such as palmitic acid, linoleic acid, α-linolenic acid, stearic acid, and sterols, which confer notable biological properties. Therefore, it is expected that the presence of such sterols in G. tournefortii may be important for its anticancer activities [10]. In vitro studies have demonstrated that kenger gum exhibits potent antibacterial activity against Escherichia coli and Streptococcus mutans, as well as cytotoxic effects on MCF-7 and 3T3 fibroblast cell lines [8]. Moreover, kenger gum has been applied in green nanotechnology as a reducing and stabilizing agent for metallic nanoparticles, enhancing their antimicrobial and anti-inflammatory efficacy [11,12] Recent investigations further reveal that kenger flowers contain the highest concentrations of bioactive compounds, display superior antioxidant activity, and exert strong antidiabetic effects via α-glucosidase and α-amylase inhibition, while maintaining low

Accepted by Scientia Iranica

cytotoxicity [11]. Gundelia tournefortii extract exhibits notable anticancer effects by inhibiting tumor growth and inducing apoptosis, highlighting its potential as a natural therapeutic agent against liver cancer [13]. Collectively, these findings position G. tournefortii gum as versatile natural biomaterials with significant biomedical potential, warranting further in-depth research.

We aimed to develop a new class of CuTiZn nanocomposite using kenger gum as a biotemplate to create an alternative to conventional antimicrobial and anticancer therapies. The synthesized nanocomposite was characterized for its structural, morphological, and chemical properties, and its antimicrobial, biofilm-inhibiting, and anticancer activities were evaluated *in vitro*. By combining the inherent properties of kenger gum with the advantageous characteristics of metal-based nanoparticles, the CuTiZn nanocomposite is expected to exhibit enhanced biological activities, making it a promising candidate for various biomedical applications.

The biosynthesized CuTiZn nanocomposite demonstrated considerable antimicrobial activity, forming inhibition zones between 13.5 and 18 mm against a range of bacterial strains. Its antioxidant potential was confirmed via DPPH radical scavenging assays, and anticancer activity was verified with an IC_{50} value of 201.1 µg/mL against the MCF-7 breast cancer cell line.

These results have a major influence on the development of new, nature-based therapeutic agents addressing the growing concerns of antibiotic resistance, chronic infections, and cancer treatment. Furthermore, the use of kenger gum as a sustainable biotemplate could enable large-scale production of these nanocomposite, offering a cost-effective and environmentally friendly alternative to current therapeutic approaches. Ultimately, this research contributes to the advancement of nanomedicine by providing an innovative, eco-friendly strategy to tackle some of the most pressing global health challenges.

2. Materials and methods

2.1. Characterization

Structural characterization was conducted by recording the X-ray diffraction patterns of the film using a Bruker A8 advanced X-ray diffractometer (XRD) with Cu Kα (0.154 nm) radiation. The surface morphologies of the materials were examined using Zeiss Supra 55 FE-SEM. The absorption spectra of the materials were obtained using a UV–Vis spectrophotometer (Shimadzu UV-2600). Fourier transform infrared (FTIR) spectroscopy was utilized in the wavenumber range of 4000–400 cm^{-1} (Perkin Elmer Spectrum400 Shimadzu, Japan). Thermogravimetric analysis (TGA) was performed with a Perkin Elmer Pyris 1 instrument, while differential thermal analysis (DTA) was conducted using a Perkin Elmer DSC 4000 apparatus.

2.2. Synthesis Process of CuO-TiO_2-ZnO (CuTiZn) ternary nanocomposite from Kenger Gum

CuTiZn nanocomposite was synthesized via a green synthesis method, in which kenger gum was used as the reducing and stabilizing agent. Kenger gum, a naturally occurring polysaccharide, was sourced locally and dissolved in distilled water to prepare a 1% (w/v) solution. The metal precursors, including copper nitrate ($Cu(NO_3)_2 \cdot 3H_2O$), titanium tetrachloride ($TiCl_4$), and zinc acetate ($Zn(CH_3COO)_2 \cdot 2H_2O$), were prepared in distilled water at a concentration of 0.01 M for each salt. A mixed solution of copper nitrate ($Cu(NO_3)_2 \cdot 3H_2O$), titanium tetrachloride ($TiCl_4$), and zinc acetate ($Zn(CH_3COO)_2$) was prepared in distilled water, each at a concentration of 0.01 M. The molar ratio of Cu:Ti:Zn was optimized to obtain the desired nanocomposite composition. The metal ion mixture was then added dropwise to the Kenger gum solution while stirring continuously, and the mixture was heated at 60°C for 2 hours. During this process, the metal ions are reduced to nanoparticles via the reducing action of kenger gum. The metal salt solution was added dropwise to the Kenger gum solution under continuous stirring. The mixture was heated at 60 °C for 2 hours, during which time the metal ions were reduced to nanoparticles by Kenger gum. The formation of nanoparticles was visually confirmed by a color change in the solution. After the reaction was complete, the mixture was allowed to cool to room temperature. After the reaction, the mixture was allowed to cool to room temperature, and the nanocomposite was separated via centrifugation at 10,000 rpm for 15 minutes. The resulting pellet was washed multiple times with distilled water to eliminate residual salts and unreacted kenger gum. The purified nanocomposite was then dried at room temperature for 48 hours to obtain the final powder form.

2.3. Examination of antimicrobial activity

The antimicrobial activities of the biosynthesized CuTiZn NCs were evaluated via the agar well diffusion method. Briefly, pathogenic bacteria (*Enterococcus faecalis* ATCC 29212, *Staphylococcus aureus* ATCC 25923,

Accepted by Scientia Iranica

Salmonella enteritidis ATCC 13075, *Enterobacter aerogenes* ATCC 13048, and *Escherichia coli* ATCC 25922) were cultured in Mueller-Hinton broth (MHB) at 37 °C and adjusted to a final concentration of 10^6 CFU/mL. After the bacterial suspension was inoculated on Mueller-Hinton agar (MHA) plates, the wells were filled with the CuTiZn nanocomposite (50 mg/mL). Following overnight incubation at 37 °C, the diameters of the inhibition zones were measured.

2.4. Determination of the minimum inhibitory concentration (MIC)

The minimal inhibitory concentration (MIC) was determined using a modified version of the Clinical and Laboratory Standards Institute (CLSI) liquid microdilution method. For standard strains, MIC testing was conducted in 96-well microplates with Mueller-Hinton Broth (MHB) as the culture medium. Following overnight incubation at 37 °C, bacterial cultures were adjusted to a concentration of 1×10^6 CFU/mL, and 100 µL of the suspension was added to each well. Subsequently, 100 µL of various concentrations (ranging from 25 to 0.39 mg/mL) of the newly synthesized CuTiZn NCs were introduced into the wells and incubated at 37 °C for 18 hours. The MIC was defined as the lowest concentration at which no visible bacterial growth was observed.

2.5. Examination of antioxidant activity

The antioxidant activity of the CuTiZn NCs was assessed via a DPPH (2,2-diphenyl-1-picrylhydrazyl hydrate) radical scavenging assay. A 0.1 mM DPPH solution was prepared, along with CuTiZn nanocomposite solutions at concentrations ranging from 50 to 0.7 mg/mL. The samples were added to a 96-well microplate and incubated in the dark for 30 minutes. Ascorbic acid was used as a positive control, and the DPPH solution alone served as a negative control. After incubation, the absorbance was measured at 517 nm via a spectrophotometer. The percentage of DPPH radical scavenging activity was calculated via the following equation:
% DPPH radical inhibition = ([(absorbance of control - absorbance of sample)/absorbance of control]) × 100.

2.6. MTT Assay

The cytotoxicity of the biosynthesized CuTiZn nanocomposite was evaluated via the MTT assay in the MCF-7 human breast cancer cell line. For cell proliferation, MCF-7 cells were cultured in Dulbecco's modified Eagle's medium (DMEM) supplemented with 10% heat-inactivated fetal bovine serum (Gibco, USA) and antibiotics (100 µg/mL streptomycin and 100 IU/mL penicillin). The cells were maintained in 75 cm^2 culture flasks at 37 °C in a humidified incubator with 5% CO_2. When the culture reached approximately 70% confluency, the cells were seeded into 96-well plates at a density of 1×10^4 cells/well and treated with various concentrations of the nanocomposite (1.81–50 mg/mL) for 24 hours. Following incubation, 10 µL of MTT solution was added to each well and incubated for an additional 3-4 hours. Afterward, the supernatant was carefully removed, and 100 µL of DMSO was added to dissolve the formazan crystals. The absorbance was measured at 570 nm via a microplate reader.

2.7. Statistical analysis

All the experiments were performed in triplicate, and the statistical analyses were conducted via GraphPad Prism version 8.0. The data are presented as the means ± standard deviations (SDs). Statistical significance was determined via Student's t test, and a p value of less than 0.05 was considered statistically significant.

3. Results and discussion

X-ray diffraction (XRD) is an essential technique used to explore the crystallographic structure, phase composition, and overall structural characteristics of materials, including nanocomposite. In this study, X-ray diffraction (XRD) was used to identify the phase composition and crystalline nature of the CuTiZn nanocomposite synthesized using kenger gum as a biotemplate (Fig. 1).

X-ray diffraction (XRD) patterns of the CuTiZn nanocomposite revealed distinct peaks corresponding to the metal oxide phases formed during synthesis. Characteristic diffraction peaks of copper oxide (CuO) were observed at 2θ values of 32.87°, 38.64°, 48.74°, and 65.96°, corresponding to the (110), (222), $(20\bar{2})$, and (022) planes, respectively (PDF Card No: 00-048-1548). Titanium dioxide (TiO_2) had peaks at 2θ = 38.64°, and 48.74°, matching the (112), and (200) planes (PDF Card No: 00-064-0863). Similarly, zinc oxide (ZnO) exhibited peaks

Accepted by Scientia Iranica

at 2θ = 32.87°, and 35.49°, which are related to the (220), and (311) planes, respectively. Copper zinc titanium oxide ($ZnCuTiO_4$) were observed at 2θ values of 35.49°, and 61.51°, corresponding to the (311), and ($11\bar{3}$) planes, respectively (PDF Card No: 00-049-0365) [14]. As shown in Table 1, the observed values are from the experiments, whereas the standard values are from PDF card reference data. The crystallite sizes were calculated via the Scherrer equation. The crystallite sizes, as determined by the calculations, ranged from 6.52 to 22.67 nanometers. The mean crystallite size was determined to be approximately 15.38 nanometers. These small differences may indicate some strain or imperfections in the crystal structure. However, the deviations are minimal and do not significantly affect the overall structure, suggesting that the CuTiZn nanocomposite maintain a well-ordered crystalline structure. These XRD results confirm that the CuTiZn nanocomposite is predominantly composed of copper oxide, titanium dioxide, and zinc oxide in their crystalline phases (Table 1). The absence of other peaks indicates that there are no significant impurities or undesired phases, suggesting that the synthesis process was relatively pure and efficient. The sharpness of the peaks further suggests well-defined crystalline structures, which are essential for ensuring the stability and enhancing the bioactivity of the nanocomposite. The crystallite size can be calculated by examining the peak widths and utilizing the Debye-Scherrer formula. The crystallite size was calculated using the Debye-Scherrer equation (Eq. 1) [15].

$$D = \frac{0.9\lambda}{\beta cos\theta} \tag{1}$$

Where λ is the X-ray wavelength (0.15406 nm for Cu Kα), θ is Bragg's diffraction angle, D is the grain size, and β is the peak's full width at half maximum (FWHM) in radians. As illustrated in Table 1, the XRD structural parameters of CuTiZn NCs are presented.

Scanning electron microscopy (SEM) analysis of the CuTiZn nanocomposite provides detailed insights into its surface morphology and the dispersion of metal nanoparticles (Fig. 2). The SEM images revealed a uniform distribution of Cu, Ti, and Zn nanoparticles within the kenger gum, with the size of the nanoparticles ranging from 5.34 to 20.34 nm. The particles exhibit a spherical shape, which is typical for nanoparticles synthesized via green synthesis methods [16]. The SEM images show that the nanoparticles are well dispersed without significant agglomeration, indicating the successful synthesis of a homogenous nanocomposite. The overall morphology suggests that the CuTiZn nanocomposite is suitable for applications that require both structural stability and efficient interaction between the metal nanoparticles. The Kenger gum provides a stable support structure, effectively dispersing the nanoparticles without any observable phase separation. Although some aggregation of the nanoparticles is observed, the overall distribution remains relatively uniform, indicating that the Kenger gum continues to provide stability. The irregular morphology of the nanoparticles may contribute to an increased surface area, potentially enhancing the material's performance in applications such as antibacterial treatments.

In conclusion, both the XRD and SEM analyses confirmed the successful synthesis of the CuTiZn nanocomposite with well-dispersed nanoparticles and distinct crystalline phases. These findings suggest that these nanocomposite possess structural integrity and stability, making them promising candidates for various technological and biomedical applications. Additionally, the elemental composition of the nanocomposite was confirmed through energy dispersive X-ray (EDX) analysis, which was performed alongside SEM imaging. Figure 3 shows the outcomes of the EDX spectrum exhibited clear peaks corresponding to copper (Cu), titanium (Ti), and zinc (Zn), which verified the successful incorporation of these metals into the nanocomposite structure (Table 2). The presence of oxygen (O) peaks further corroborated the formation of metal oxide phases, which is consistent with the XRD results.

In summary, SEM analysis provided essential insights into the morphology and structural properties of the CuTiZn nanocomposite. The uniform particle distribution, spherical morphology, and lack of aggregation are indicative of a successful synthesis process and the stabilization of the nanoparticles. These findings are consistent with the results from the XRD and EDX analyses, confirming the incorporation of copper, titanium, and zinc into the nanocomposite structure. The well-dispersed nanoparticles observed in this study are critical for the potential biomedical applications of these nanocomposite, as they ensure effective interactions with biological systems.

The transmittance data provide valuable insights into the optical properties of the material, which are particularly relevant for potential biological applications, such as antibacterial and anticancer treatments. These findings suggest that the material interacts effectively with light, a characteristic that could be utilized in antibacterial applications, where light is often employed to inactivate microorganisms.

The optical transmittance spectrum of the material was measured in the wavelength range of 400–700 nm, as presented in Figure 4. The transmittance values exhibit a gradual and nearly linear increase across the visible region, indicating a progressive reduction in light absorption with increasing wavelength. At 400 nm, the transmittance value was approximately 24.1%, while it increased steadily to reach nearly 38.1% at 700 nm. This

Accepted by Scientia Iranica

suggests that the material allows some light penetration, potentially facilitating deeper tissue interactions in anticancer applications. This feature could be particularly beneficial for treatments such as photodynamic therapy, where effective light penetration into deeper tissues is crucial for targeting cancer cells. The moderate transmittance at these wavelengths indicates that the material can interact with tissues while allowing enough light to reach the target area.

The optical band width (E_g) values of the CuO NPs were calculated by extrapolating a linear relationship between the $(\alpha hv)^2$ and photon energy (hv) curves to the energy axis when $(\alpha hv)^2 = 0$, as shown in Fig. 5. The variation in α with hv is given by the power law of Tauc's relation (Tauc, 1974) [17].

$$(\alpha hv) = C(hv - E_g)^n \quad (2)$$

where C is a constant, hv is the incident photon energy, and n represents the transition type. For an allowed direct transition, n is equal to ½, whereas for an allowed indirect transition, n is equal to 2.
The energy band gap calculated from the plot of $(\alpha hv)^2$ as a function of photon energy (hv) was found to be 2.93 eV.

Fourier transform infrared spectroscopy (FTIR) was employed to identify the functional groups involved in the interaction between the metal ions and kenger gum. The spectra showed characteristic absorption peaks associated with functional groups in kenger gum, such as hydroxyl (–OH) and carbonyl (C=O) groups. These groups play a significant role in stabilizing the metal nanoparticles. The FTIR spectra also displayed shifts in characteristic bands, indicating the interaction between the kenger gum and the metal nanoparticles, thereby confirming the formation of the CuTiZn nanocomposite (Fig. 6). The FTIR spectrum of the CuTiZn nanocomposite exhibited several characteristic peaks, corresponding to various functional groups and bonding structures. A broad absorption band at approximately 3400 cm^{-1} was observed, which is typically associated with the stretching vibrations of the O–H bond. This broad peak indicates the presence of hydroxyl groups, which may originate from both kenger gum and the metal oxide surfaces. This feature is characteristic of polysaccharides, suggesting that kenger gum plays a stabilizing role in the synthesis of metal nanoparticles. The distinct peak at approximately 1620 cm^{-1} was attributed to the bending vibrations of the C–H bond, indicating the presence of residual organic material from Kenger gum, which was likely incorporated into the nanocomposite during synthesis. This observation further supports the hypothesis that the biotemplate is integral to the formation and structural integrity of the nanocomposite. Additionally, absorption bands in the range of 500–700 cm^{-1} were identified, corresponding to metal–oxygen (M–O) stretching vibrations. These peaks are characteristic of metal oxide phases, confirming the formation of CuO, TiO_2, and ZnO nanoparticles, in agreement with the results obtained from X-ray diffraction (XRD) analysis. The observed vibrations specifically correspond to Cu–O, Ti–O, and Zn–O bonds, further validating the successful synthesis of the CuTiZn nanocomposite and their metal oxide composition. Another peak at approximately 1050 cm^{-1} was attributed to C–O stretching vibrations, suggesting the presence of glycosidic bonds or other carbohydrate-related functional groups derived from kenger gum [18]. Notably, the FTIR spectrum did not exhibit any significant peaks indicative of unwanted byproducts or impurities, suggesting that the green synthesis approach employing kenger gum effectively yields relatively pure nanocomposite. The identified functional groups and their interactions with the metal nanoparticles are fundamental to the stability and bioactivity of the nanocomposite, highlighting their potential for biomedical applications.

In conclusion, FTIR analysis provided significant insights into the functional groups present in the CuTiZn nanocomposite, as well as the interactions between kenger gum and the metal nanoparticles. The results confirmed the successful incorporation of metal oxides (CuO, TiO_2, ZnO) into the nanocomposite structure and highlighted the stabilizing role of kenger gum. The identified functional groups, including hydroxyl, C-H, and C-O groups, are indicative of the stabilizing and structuring influence of the biotemplate, further supporting the suitability of these nanocomposite for potential biomedical applications.

Thermogravimetric analysis (TGA) and differential thermal analysis (DTA) were conducted to evaluate the thermal stability, decomposition behavior, and phase transitions of the CuTiZn nanocomposite synthesized using kenger gum as a biotemplate (Fig. 7). TGA measures the mass loss of a material as a function of temperature, whereas DTA records the temperature difference between a sample and a reference material during heating. The TGA curve of the CuTiZn nanocomposite exhibited a distinct multistep weight-loss pattern, reflecting various stages of thermal decomposition. An initial weight loss of approximately 3–5% was observed between 25 and 150°C, corresponding to the evaporation of adsorbed moisture and residual solvents such as water [19]. No significant weight loss occurred until higher temperatures, indicating that both the metal nanoparticles and Kenger gum remained stable at lower temperatures. A more pronounced weight loss of about 15–20% was recorded between 200 and 350°C, primarily attributed to the thermal degradation of the organic components, particularly the kenger gum. The polysaccharide structure of kenger gum decomposed at elevated temperatures, releasing volatile carbon-containing compounds. Despite this degradation, the overall thermal stability of the metal oxide

Accepted by Scientia Iranica

nanoparticles remained largely unaffected. The TGA results indicated that CuTiZn nanocomposite exhibited high thermal stability, with minimal weight loss observed at temperatures ranging from 400–500°C. The DTA curves revealed endothermic peaks associated with the melting of metal nanoparticles and exothermic peaks related to polymer decomposition. These findings confirm that the CuTiZn nanocomposite possesses high thermal stability and can withstand elevated temperatures, making it suitable for applications requiring thermal resilience.

The DTA results are consistent with the findings from the TGA analysis, particularly regarding the decomposition of kenger gum and the thermal stability of the metal oxide phases. Both analyses support the conclusion that the CuTiZn nanocomposite exhibits excellent thermal stability, with minimal weight loss attributable to the decomposition of organic residues. These results highlight the robustness of the nanocomposite at elevated temperatures.

NCs have gained significant attention in recent studies as potential therapeutic agents for the treatment of various diseases. Numerous investigations have demonstrated that nanoparticles possess potent antimicrobial properties and may serve as alternative treatment strategies to combat the growing issue of antimicrobial resistance. The antimicrobial mechanism of nanoparticles is attributed primarily to the generation of reactive oxygen species (ROS) within microbial cells triggered by the release of metal ions. ROS induce oxidative stress, leading to damage to vital biomolecules such as proteins, lipids, and DNA, ultimately resulting in cell death [20]. The antibacterial activity of the biosynthesized CuTiZn ternary nanocomposite is primarily attributed to the generation of reactive oxygen species (ROS), which disrupt bacterial cell membranes, proteins, and DNA. The multifunctional activity of CuTiZn nanocomposite arises from a combination of physical interaction with cell membranes, ROS-mediated oxidative damage, and metal ion interference with cellular processes, which collectively confer potent antibacterial and cytotoxic properties [21,22]. Previous studies on Gundelia tournefortii gum have highlighted its significant anticancer potential, particularly against HCT-116 colon cancer cells, where methanolic and hexane extracts demonstrated marked cytotoxic activity while the aqueous extract remained inactive. The GC–MS analysis revealed the presence of several bioactive phytochemicals such as sitosterol, stigmasterol, lupeol, gitoxigenin, α-amyrin, and artemisinin, which are known to modulate multiple molecular targets involved in apoptosis and oxidative stress regulation. These compounds are suggested to induce mitochondrial-mediated apoptosis by increasing intracellular reactive oxygen species (ROS) levels, triggering caspase activation, and leading to DNA fragmentation and cell cycle arrest. In the current study, the incorporation of G. tournefortii gum as a biogenic reducing and stabilizing agent in the synthesis of the ternary CuO–TiO_2–ZnO (CuTiZn) nanocomposite not only enhances the structural and surface properties of the material but also amplifies its biological activity. The synergistic interaction between the phytochemical components and the metallic oxides is expected to promote reactive oxygen species generation and disruption of cancer cell membranes, contributing to the observed antibacterial and anticancer activities. Therefore, the CuTiZn nanocomposite synthesized using G. tournefortii gum represents a promising multifunctional material with potential biomedical applications, particularly in targeted cancer therapy and antimicrobial systems [10].

In the present study, the antimicrobial activity of CuTiZn nanocomposite (NCs), synthesized via a green approach using *Gundelia tournefortii* (Kenger) gum, was evaluated against both Gram-positive (*Enterococcus faecalis*, *Staphylococcus aureus*) and Gram-negative (*Enterobacter aerogenes*, *Salmonella enteritidis*, *Escherichia coli*) pathogenic strains, with gentamicin serving as a positive control (Fig. 8a). The biosynthesized nanocomposite exhibited inhibition zones ranging from 13.5 to 18 mm, compared to 14–21 mm observed for gentamicin (Fig. 8b). Among the tested strains, *E. coli* was the most susceptible, whereas *E. aerogenes* showed the lowest sensitivity. The minimum inhibitory concentration (MIC) of CuTiZn NCs was determined to be between 0.78 and 1.56 mg/mL (Table 3).

Recently, green synthesis of CuO, TiO_2, and ZnO-based nanocomposite has attracted increasing attention due to their notable antibacterial and cytotoxic properties. Several studies have reported enhanced biological activities arising from the synergistic interactions of combined metal oxides. For instance, Papitha et al. (2024) demonstrated that CuO/TiO_2 and ZnO/TiO_2 nanocomposite synthesized using *Parkia timoriana* bark extract exhibited significant antioxidant and antidiabetic activities, highlighting the promise of these materials for biomedical applications [23]. Similarly, Wong et al. (2024) reported that CuO/ZnO nanocomposite synthesized from *Musa acuminata* leaf extract exerted cytotoxic effects against colorectal cancer cells, with particle sizes ranging from 31.8 to 85.7 nm and a bandgap of 3.43 eV [24]. Moreover, El-Sawaf et al. (2024) synthesized CuO/Ag/ZnO nanocomposite using *Ziziphus spina christi* leaves, which displayed spherical structures (~7.11 ± 0.67 nm) and a zeta potential of 21.5 mV, demonstrating remarkable antimicrobial activity against multidrug-resistant pathogens, including *E. coli* and *S. aureus*, with biofilm reduction exceeding 97% [25]. These observations strongly align with our findings, as the CuO-TiO_2-ZnO (CuTiZn) ternary nanocomposite synthesized via Kenger gum extract similarly exhibited potent antibacterial and cytotoxic activities. The enhanced efficacy can be attributed to the synergistic interactions among CuO, TiO_2, and ZnO, further augmented by bioactive phytochemicals present in the Kenger gum extract. Collectively, these results demonstrate the applicability of green-synthesized CuTiZn nanocomposite as sustainable and highly effective candidates for diverse biomedical applications.

Accepted by Scientia Iranica

Overall, the antimicrobial activity of the CuTiZn NCs was noteworthy compared with that of the standard antibiotic control. These findings suggest that CuTiZn NCs, which were successfully synthesized via an eco-friendly method, possess promising bactericidal properties and could be considered potential candidates for biomedical applications.

Copper oxide nanoparticles (CuO-NPs) synthesized from extracts of *Athrixia phylicoides* have demonstrated significant antibacterial activity, particularly against *Bacillus cereus* and *Staphylococcus aureus* [26]. Similarly, TiO_2 nanoparticles prepared from *Laurus nobilis* leaf extract exhibited antimicrobial properties against both gram-positive and gram-negative bacteria, with the largest inhibition zone observed for *Bacillus subtilis* (16 mm), followed by *E. coli* (15 mm) and *Klebsiella pneumoniae* (13 mm) [10]. Zinc oxide nanoparticles (ZnO-NPs) biosynthesized from *Punica granatum* at a concentration of 100 µg/mL produced inhibition zones ranging from 15 to 20 mm against *B. subtilis*, *S. aureus*, *P. aeruginosa*, and *E. coli* [27]. In another study, the antibacterial activities of the biosynthesized CuO NPs, ZnO NPs, 10% CuO/ZnO, and 20% CuO/ZnO nanocomposite was tested against *S. aureus* and *E. coli*. The 20% CuO/ZnO nanocomposite exhibited the highest inhibitory activity, which was attributed to the synergistic interaction of the constituent nanoparticles [28]. In line with these findings, it is hypothesized that the CuTiZn nanocomposite synthesized in the present study also exhibit a synergistic antimicrobial effect due to the combined action of CuO, TiO_2, and ZnO nanoparticles.

Antioxidants play a critical role in cellular defense by neutralizing reactive oxygen species (ROS), which are known to cause oxidative damage to biomolecules. The antioxidant properties of biosynthesized nanocomposite is largely attributed to both the intrinsic redox activity of metal oxides and the presence of phytochemicals derived from plant extracts [29,30]. Metal ions within the nanocomposite can interact with ROS, reducing their reactivity and mitigating oxidative stress. Additionally, phytoconstituents contribute significantly to antioxidant capacity because of their electron-donating ability and free radical scavenging mechanisms. Several factors including the chemical composition, surface charge, crystal structure, and particle size of the nanocomposite can influence their overall antioxidant performance [31].

The antioxidant activity of the CuTiZn nanocomposite synthesized from *Gundelia tournefortii* (Kenger) gum is presented in Fig. 9. The IC_{50} value of the nanocomposite was calculated to be 22.82 mg/mL. At a concentration of 12.5 mg/mL, the DPPH radical scavenging efficiency of the nanocomposite was approximately 34%, with activities ranging between 17% and 34% across the tested concentrations. While this activity is lower than that of the positive control (ascorbic acid), which showed an average inhibition of ~90%, it nonetheless demonstrates the antioxidant potential of the CuTiZn NCs.
In comparison, CuO nanoparticles synthesized using *Ligustrum lucidum* extract exhibited 38.62% inhibition at 50 µg/mL [32], TiO_2 NPs reached 46.71% inhibition at 200 µg/mL [26], and ZnO NPs showed approximately 70% inhibition at 100 µg/mL [33]. Although the CuTiZn NCs in this study required relatively high concentrations to achieve similar or low activity levels, the observed antioxidant effects may be influenced by factors such as the particle size, surface charge, chemical composition, or crystalline structure of the nanocomposite.

Cytotoxicity refers to the ability of a substance to affect cell viability and metabolic activity and induce cell death, and it is a key parameter in assessing the biomedical potential of nanomaterials. The MTT assay is one of the most widely used methods to evaluate cytotoxicity by measuring mitochondrial activity. Additionally, the cytotoxic effects of CuTiZn nanocomposite synthesized with *Gundelia tournefortii* (kenger) gum as a reducing and stabilizing agent were investigated in the MCF-7 human breast cancer cell line.

The nanocomposite was tested over a concentration range of 0.5-5000 µg/mL. At concentrations of 5000 and 500 µg/mL, the CuTiZn NCs induced approximately 90% cell death, indicating statistically significant cytotoxicity ($p < 0.0001$). At 50 µg/mL, the nanocomposite inhibited cell viability by approximately 30%. The half-maximal inhibitory concentration (IC_{50}) value was calculated as 201.1 µg/mL. These results demonstrate that the CuTiZn NCs exhibit potent dose-dependent cytotoxic activity against MCF-7 cells (Fig. 10).

Several studies have reported the cytotoxic effects of green-synthesized metal oxide nanocomposite on different cancer cell lines. For example, CuO/ZnO nanocomposite exhibited 45.79% cytotoxicity at 100 µg/mL against HCC2998 colorectal cancer cells [24]. In MCF-7 human breast cancer cells, 50% CuO/ZnO nanocomposite induced approximately 60% cell death at the same concentration, with an IC_{50} value of 78.9 µg/mL [34]. CuO/TiO_2-chitosan-farnesol nanocomposite demonstrated a much stronger effect on SK-MEL-3 melanoma cells, with an IC_{50} of 12.5 µg/mL [35,36]. Another study reported an IC_{550} value of 282.4 µg/mL for ZnO NPs in colorectal cancer cells, where treatment at this dose significantly upregulated the expression of the p53 and Casp3 genes by 1.22-fold and 3.81-fold, respectively [37]. In MCF-7 cells, TiO_2 nanoparticles were found to have an IC_{50} of 120 µg/mL and exhibited notable anticancer activity [38]. Compared with the literature, although the IC_{50} value of the biosynthesized CuTiZn nanocomposite in the present study was relatively high (201.1 µg/mL), the results still indicate notable anticancer activity. It is hypothesized that prolonged exposure (48-72 hours) may enhance their cytotoxic effect on MCF-7 cells.

4. Conclusion

Accepted by Scientia Iranica

In this study, a CuO–TiO_2–ZnO (CuTiZn) ternary nanocomposite was successfully synthesized using *Gundelia tournefortii* (kenger) gum extract as a natural biotemplate and reducing agent. This eco-friendly, cost-effective, and straightforward green synthesis route eliminated the need for hazardous chemicals while ensuring high stability and reproducibility. Kenger gum, a natural polysaccharide known for its abundant availability and nontoxic nature, was employed as a sustainable biotemplate for the green synthesis of the CuTiZn-based nanocomposite. The structural, morphological, and thermal properties were investigated through several characterization techniques, while the antimicrobial and anticancer activities were systematically evaluated. Comprehensive characterization analyses, including XRD, SEM, EDX, FTIR, TGA, and DTA, confirmed the formation of a well-defined, crystalline, and spherical nanocomposite with excellent structural and thermal properties.

The biosynthesized CuTiZn nanocomposite demonstrated remarkable antibacterial, antioxidant, and anticancer activities. It exhibited a maximum antibacterial inhibition zone of 18 mm against *Escherichia coli*, outperforming many previously reported TiO_2/ZnO or CuO-based nanocomposite. The DPPH radical scavenging assay indicated an inhibition rate of approximately 34% at 12.5 mg/mL, reflecting significant antioxidant potential. Moreover, cytotoxicity assays revealed a half-maximal inhibitory concentration (IC_{50}) of 201.1 µg/mL against the MCF-7 human breast cancer cell line, highlighting promising anticancer efficacy.

These enhanced biological activities are attributed to the synergistic effects of CuO, TiO_2, and ZnO metal oxides, combined with the stabilizing and biocompatible coating provided by kenger gum. When compared to similar green-synthesized metal oxide systems, the CuTiZn nanocomposite exhibits superior biological performance and an improved sustainability profile, underscoring its scientific novelty and environmental significance.

In conclusion, the biosynthesized CuTiZn nanocomposite represents a versatile and multifunctional material with strong potential for biomedical and environmental applications. Future research should focus on optimizing synthesis parameters, exploring photocatalytic performance, drug delivery potential, and tissue compatibility to fully harness its therapeutic capabilities. Collectively, these findings position the CuTiZn nanocomposite as a promising candidate for advanced biomedical applications due to its robust antimicrobial, antioxidant, and anticancer properties.

Acknowledgements

No data was used for the research described in the article.

We thank Dr. Esen ÇAKMAK (Kahramanmaraş Sütçü İmam University) for the help with the application of antimicrobial and biological studies.

Author contributions

Saniye Tekerek: Conceptualization; Methodology; Investigation; Visualization; Writing-original draft; Validation; Writing-review and editing.

Funding

This research did not receive any specific grant from funding agencies in the public, commercial, or not-for-profit sectors.

Conflicts of interest

The authors declare that they have no known competing financial interests or personal relationships that could have appeared to influence the work reported in this paper.

Data availability

The data that support the findings of this study are available from the corresponding author upon reasonable request.

References

Accepted by Scientia Iranica

1. Jalal, M., Ansari, M.A., Alzohairy, M.A., et al. “Biosynthesis of Silver Nanoparticles from Oropharyngeal Candida Glabrata Isolates and Their Antimicrobial Activity against Clinical Strains of Bacteria and Fungi”, *Nanomaterials*, 8(8), pp. 586 (2018). https://doi.org/10.3390/nano8080586

2. Lee, K.D. and Nagajyothi, P.C. “Synthesis of Plant-Mediated Silver Nanoparticles Using Dioscorea Batatas Rhizome Extract and Evaluation of Their Antimicrobial Activities”, *Journal of Nanomaterials*, 2011(1), pp. 573429 (2011). https://doi.org/10.1155/2011/573429

3. Singh, J., Dutta T., Kim, K.H., et al. “Green Synthesis of Metals and Their Oxide Nanoparticles: Applications for Environmental Remediation”, *Journal of Nanobiotechnology*, 16(84), pp. 1–25 (2018). https://doi.org/10.1186/s12951-018-0408-4

4. Ishaque, M.Z., Zaman, Y., Arif, A., et al. “Fabrication of ternary metal oxide (ZnO:NiO:CuO) nanocomposite heterojunctions for enhanced photocatalytic and antibacterial applications”, *RSC Advances*, 13(44), pp. 30838–30854 (2023). DOI: 10.1039/D3RA05170F

5. Rajendran, R., Rojviroon, O., Arumugam, P., et al. “Synergistic effects of activated Carbon-Supported TiO2/ZnO nanocomposites for photocatalytic dye degradation and antibacterial activity”, *Journal of Molecular Liquids*, 433, 127792, pp. 1-11 (2025). https://doi.org/10.1016/j.molliq.2025.127792

6. Boonwan, C., Rojviroon, T., Rojviroon, O., et al. “Micro-nano bubbles in action: AC/TiO2 hybrid photocatalysts for efficient organic pollutant degradation and antibacterial activity”, *Biocatalysis and Agricultural Biotechnology*, *61*, 103400 (2024). https://doi.org/10.1016/j.bcab.2024.103400

7. Rajendran, R., Alsawalha, M., Alomayri, T., et al. “Optimized MoS2/SnS2@ AC nanocomposites for superior visible light-driven pollutant degradation and antibacterial activity”, *Inorganic Chemistry Communications*, *173*, 113839, (2025). https://doi.org/10.1016/j.inoche.2024.113839

8. Topcuoglu, N., Lacin, C.C., Erguven, M., et al. “Antibacterial effect of kenger gum on mutans streptococci and its cytotoxic effect on the 3T3 fibroblast cell line”, *Oral Health Prev. Dent.*, 13(2), pp. 157–162 (2015). doi: 10.3290/j.ohpd.a32666

9. Hani, N., Abulaila, K., Howes, M.J., et al. “Gundelia tournefortii L.(Akkoub): A review of a valuable wild vegetable from Eastern Mediterranean”, *Genetic Resources and Crop Evolution*, 71(8), pp. 3987–3995 (2024). https://doi.org/10.1007/s10722-024-01927-2

10. Abu-Lafi, S., Rayan, B., Kadan, S., et al. “Anticancer activity and phytochemical composition of wild Gundelia tournefortii”, *Oncology letters*, *17*(1), pp. 713-717(2019). https://doi.org/10.3892/ol.2018.9602

11. Kutlu, G. and Erol, K.F. “An in vitro assessment of the bioactive, cytotoxic, and antidiabetic potential of different parts of tumbleweed (Gundelia tournefortii L.) ”, *Gıda*, 50(1), pp. 28–41 (2025). https://doi.org/10.15237/gida.GD24096

12. Keskin, C., Baran, A., Baran, M.F., et al. “Green synthesis, characterization of gold nanomaterials using Gundelia tournefortii leaf extract, and determination of their nanomedicinal (antibacterial, antifungal, and cytotoxic) potential”, (1), pp. 7211066 (2022). https://doi.org/10.1155/2022/7211066

13. Amer, J., Jaradat, N., Aburas, H., et al. “Gundelia Tournefortii extracts inhibit progressions of Hepatocellular Carcinoma in mice model through decrease in p53/Akt/PI3K signaling pathway”, pp. 1-16 (2020). https://doi.org/10.21203/rs.3.rs-97723/v1

14. Tseng, Y.W., and Huang, C.L. “Sintering behavior and microwave dielectric properties of ZnCuTiO4 ceramics”, *Journal of Alloys and Compounds*, 638, pp. 29-33 (2015). https://doi.org/10.1016/j.jallcom.2015.03.067

15. Stokes, A.R. and Wilson, A.J.C. “The diffraction of X rays by distorted crystal aggregates-I”, *Proceedings of the Physical Society*, 56(3), pp. 174 (1944).

16. Maheswari, P., Sugapriya, S., Krishnaveni, N., et al. “Investigation of Pure and CuO-and ZnO-Loaded TiO2 Nanocomposites Prepared by Modified Hydrothermal Cum Green Synthesis (Hybanthus enneaspermus Extract) Method for Photocatalytic and Antioxidant Applications”, *Brazilian Journal of Physics*, 52(4), pp. 142 (2022). https://doi.org/10.1007/s13538-022-01112-9

17. Tauc, J., *Amorphous and Liquid Semiconductors*, Plenum Press, New York (1974).

18. Ilpo, N., Forsberg, V., Zakrisson, D., et al. “Determination of Nanoparticle Size Using Rayleigh Approximation and Mie Theory”, *Chemical Engineering Science*, 201, pp. 222–229 (2019). https://doi.org/10.1016/j.ces.2019.02.020

Accepted by Scientia Iranica

19. Khalid, R., Raza, S., Areej, I., et al. “Green Synthesis of Nickel Oxide Nanoparticles from Lawsonia inermis Leaf Extract for Promising Methyl Red Uptake and Efficient Iodine Adsorption”, (Early Access), pp. 1–36 (2024). https://doi.org/10.21203/rs.3.rs-4439351/v1

20. Rajeswari, V.D., Eed, E.M., Elfasakhany, A., et al. “Green synthesis of titanium dioxide nanoparticles using Laurus nobilis (bay leaf): Antioxidant and antimicrobial activities”, *Applied Nanoscience*, pp. 1–8 (2021). https://doi.org/10.1007/s13204-021-02065-2

21. Vasiliev, G., Kubo, A.L., Vija, H., et al. “Synergistic antibacterial effect of copper and silver nanoparticles and their mechanism of action”, *Scientific Reports*, *13*(1), 9202, (2023). https://doi.org/10.1038/s41598-023-36460-2

22. Hao, Z., Wang, M., Cheng, L., et al. “Synergistic antibacterial mechanism of silver-copper bimetallic nanoparticles”, *Frontiers in Bioengineering and Biotechnology*, *11*, pp. 1337543, (2024). https://doi.org/10.3389/fbioe.2023.1337543

23. Papitha, R., Hadkar, V., Sishu, N.K., et al. “Green synthesis of CuO/TiO2 and ZnO/TiO2 nanocomposites using Parkia timoriana bark extract: Enhanced antioxidant and antidiabetic activities for biomedical applications”, *Ceramics International*, *50*(20), 39109-39121, (2024). https://doi.org/10.1016/j.ceramint.2024.07.277

24. Wong, Y.J., Subramaniam, H., Shing Wong, L., et al. “Green synthesis and characterization of CuO/ZnO nanocomposite using *Musa acuminata* leaf extract for cytotoxic studies on colorectal cancer cells (HCC2998)”, *Green Processing and Synthesis*, 13(1), pp. 20240164 (2024). https://doi.org/10.1515/gps-2024-0164

25. El-Sawaf, A.K., El-Moslamy, S.H., Kamoun, E.A., et al. “Green synthesis of trimetallic CuO/Ag/ZnO nanocomposite using Ziziphus spina-christi plant extract: characterization, statistically experimental designs, and antimicrobial assessment”, *Scientific Reports*, *14*(1), pp.19718, (2024). https://doi.org/10.1038/s41598-024-67579-5

26. Kaningini, A.G., Motlhalamme, T., More, G.K., et al. “Antimicrobial, antioxidant, and cytotoxic properties of biosynthesized copper oxide nanoparticles (CuO-NPs) using *Athrixia phylicoides* DC”, *Heliyon*, 9(4) (2023). DOI: 10.1016/j.heliyon.2023.e15265

27. Fouda, A., Saied, E., Eid, A.M., et al. “Green synthesis of zinc oxide nanoparticles using an aqueous extract of *Punica granatum* for antimicrobial and catalytic activity”, *Journal of Functional Biomaterials*, 14(4), pp. 205 (2023). https://doi.org/10.3390/jfb14040205

28. Takele, E., Feyisa Bogale, R., Shumi, G., et al. “Green synthesis, characterization, and antibacterial activity of CuO/ZnO nanocomposite using *Zingiber officinale* rhizome extract”, *Journal of Chemistry*, 2023(1), pp. 3481389 (2023). https://doi.org/10.1155/2023/3481389

29. Cuong, H.N., Pansambal, S., Ghotekar, S., et al. “New frontiers in the plant extract mediated biosynthesis of copper oxide (CuO) nanoparticles and their potential applications: A review”, *Environmental Research*, 203, pp. 111858 (2022). https://doi.org/10.1016/j.envres.2021.111858

30. Nguyen, T.T.T., Nguyen, Y.N.N., Tran, X.T., et al. “Green synthesis of CuO, ZnO and CuO/ZnO nanoparticles using *Annona glabra* leaf extract for antioxidant, antibacterial and photocatalytic activities”, *Journal of Environmental Chemical Engineering*, 11(5), pp. 111003 (2023). https://doi.org/10.1016/j.jece.2023.111003

31. Malik, K., Kazmi, A., Sultana, T., et al. “A mechanistic overview on green assisted formulation of nanocomposites and their multifunctional role in biomedical applications”, *Heliyon*, 11(3) (2025). DOI: 10.1016/j.heliyon.2025.e41654

32. Ogwuegbu, M.C., Ayangbenro, A.S., Mthiyane, D.M., et al. “Green synthesis of CuO nanoparticles using *Ligustrum lucidum* extract, and the antioxidant and antifungal evaluation”, *Materials Research Express*, 11(5), pp. 055010 (2024). DOI: 10.1088/2053-1591/ad4e9d

33. Abdelbaky, A.S., Abd El-Mageed, T.A., Babalghith, A.O., et al. “Green synthesis and characterization of ZnO nanoparticles using *Pelargonium odoratissimum* (L.) aqueous leaf extract and their antioxidant, antibacterial and anti-inflammatory activities”, *Antioxidants*, 11(8), pp. 1444 (2022). https://doi.org/10.3390/antiox11081444

34. Fathima Fasna, P.H., Sasi, S., Julie Chandra, C.S., et al. “Green Synthesis of CuO/ZnO Nanocomposites using *Ficus drupacea*: In-Vitro Antibacterial and Cytotoxicity Analysis”, *ChemistrySelect*, 9(22), pp. e202401235 (2024). https://doi.org/10.1002/slct.202401235

Accepted by Scientia Iranica

35. Indumathi, T., Suriyaprakash, J., Alarfaj, A.A., et al. “Synergistic effects of CuO/TiO_2-chitosan-farnesol nanocomposites: synthesis, characterization, antimicrobial, and anticancer activities on melanoma cells SK-MEL-3”, *Journal of Basic Microbiology*, 64(2), pp. 2300505 (2024). https://doi.org/10.1002/jobm.202300505

36. Sanaeimehr, Z., Javadi, I., and Namvar, F. “Antiangiogenic and antiapoptotic effects of green-synthesized zinc oxide nanoparticles using *Sargassum muticum* algae extraction”, *Cancer Nanotechnology*, 9(3), pp. 1–16 (2018). https://doi.org/10.1186/s12645-018-0037-5

37. Sabet, B.J.P., Mahdavi-Ourtakand, M., and Baghbani-Arani, F. “Green synthesis of zinc oxide nanoparticles by *Zataria multiflora* extract and evaluation of its antimicrobial, cytotoxic and apoptotic effects on HT-29 cell line”, *Koomesh*, 24(3), pp. 388–396 (2022). http://koomeshjournal.semums.ac.ir/article-1-7015-en.pdf

38. Venkatappa, M.M., Udagani, C., Hanume Gowda, S.M., et al. “Green synthesized TiO_2 nanoparticles-mediated *Terenna asiatica*: evaluation of their role in reducing oxidative stress, inflammation and human breast cancer proliferation”, *Molecules*, 28(13), pp. 5126 (2023). https://doi.org/10.3390/molecules28135126

Biography

Saniye Tekerek obtained her M.Sc. degree in 2009 from Sütçü İmam University, Kahramanmaraş, Turkey. She received her Ph.D. in Science in 2019 from the same university. In 2025, she was awarded the title of Associate Professor. Presently, she is working as an associate professor in the Department of Medical Services and Techniques, Kahramanmaraş Sütçü İmam University, Vocational School of Health Services, Turkey. Her area of specialization is the synthesis of metal oxides for photovoltaic applications, and she primarily works in the field of semiconductor thin films and nanostructures. In addition, she conducts research on antibacterial materials.

Figure Captions

Figure 1. XRD pattern of CuTiZn NCs produced from Kenger gum.

Figure 2. SEM image of a KG CuTiZn NCs taken at magnifications of a) 400.00 K × , b)200.00 K ×, c) 100.00 K ×, d) 50.00 K ×, and e) 25.00 K ×

Figure 3. EDX spectra of the ternary CuTiZn nanocomposite.

Figure 4. The transmittance graphs of CuTiZn NCs.

Figure 5. Plot of $(\alpha h\nu)^2$ and photon energy $(h\nu)$ for the CuTiZn NCs.

Figure 6. FTIR spectrum of CuTiZn NCs.

Figure 7. DTA-TGA spectrum of CuTiZn NCs.

Figure 8. Antimicrobial activity of CuTiZn nanocomposite synthesized from *G. tournefortii* (kenger) gum. a) Representative image of inhibition zones for each pathogen, b) Quantitative comparison of inhibition zone diameters (mm) for each pathogen.

Figure 9. Antioxidant activity of the CuTiZn nanocomposite synthesized from *G. tournefortii* (kenger) gum, as evaluated via a DPPH radical scavenging assay.

Figure 10. Cytotoxic activity of the CuTiZn nanocomposite synthesized with *G. tournefortii* (kenger) gum against MCF-7 breast cancer cells, as assessed via the MTT assay.

Table Captions

Table 1. XRD structural parameters of CuTiZn NCs.

Table 2. EDX spectral parameters of the CuTiZn nanocomposite.

Table 3. Antibacterial activity of CuTiZn NCs produced from Kenger gum on pathogenic strains.

Accepted by Scientia Iranica

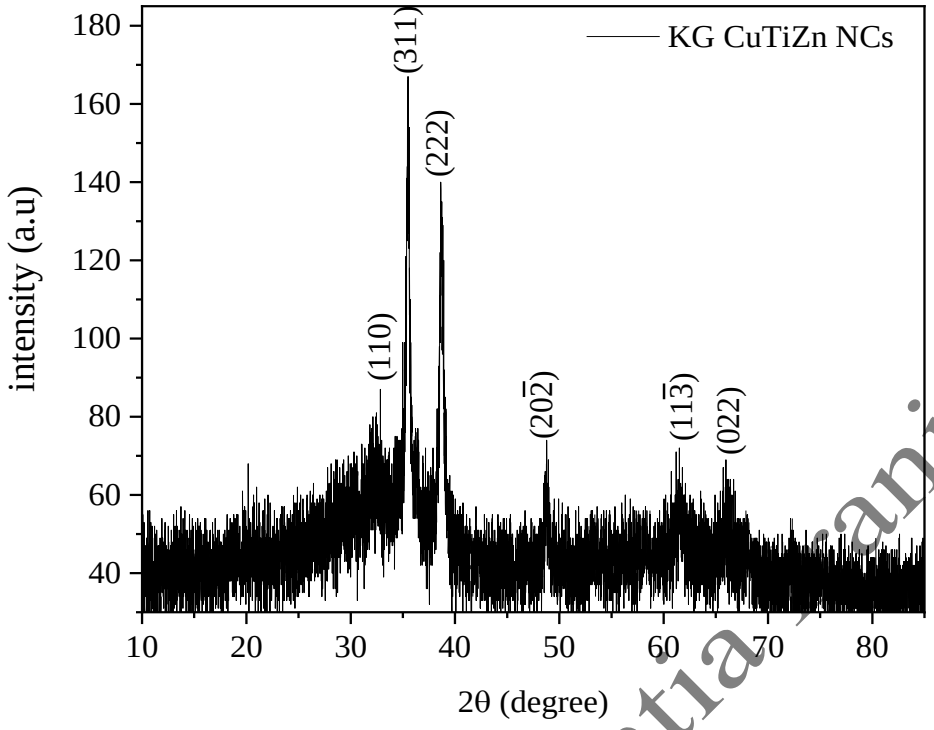

Figure 1. XRD pattern of CuTiZn NCs produced from Kenger gum.

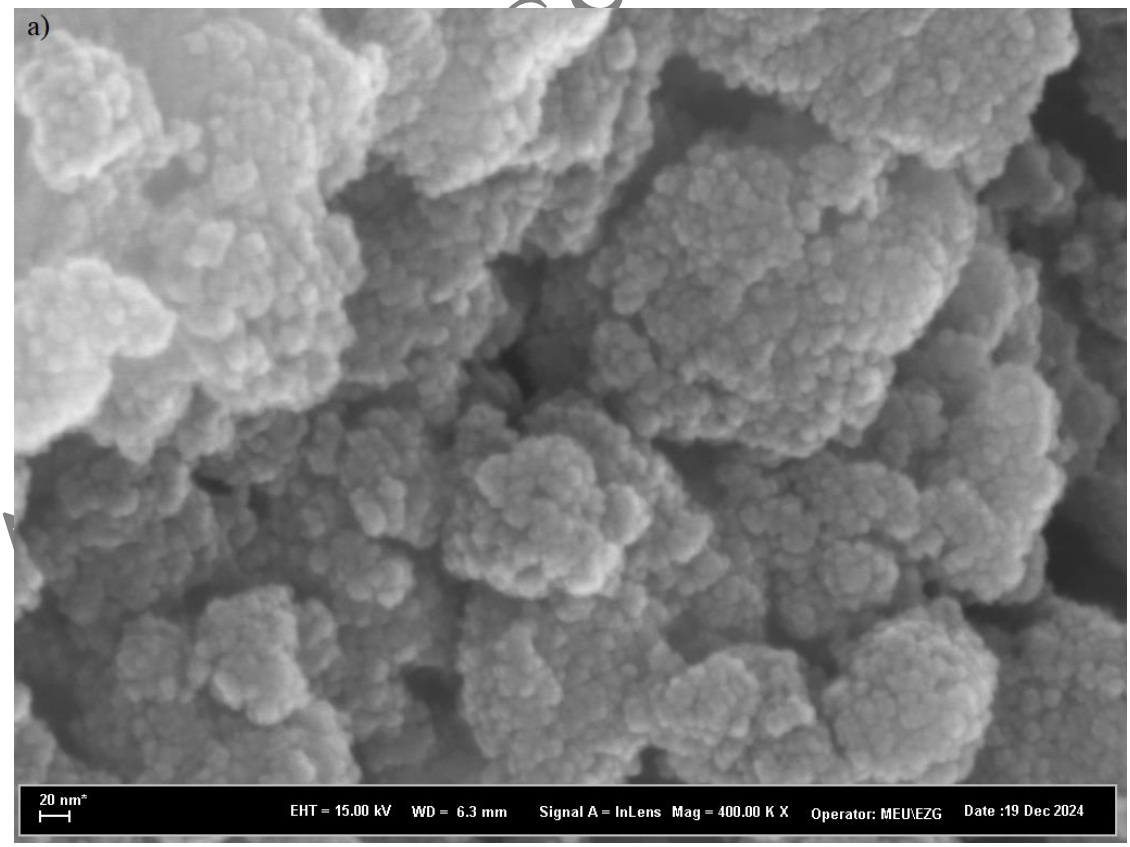

Scientia Islamica

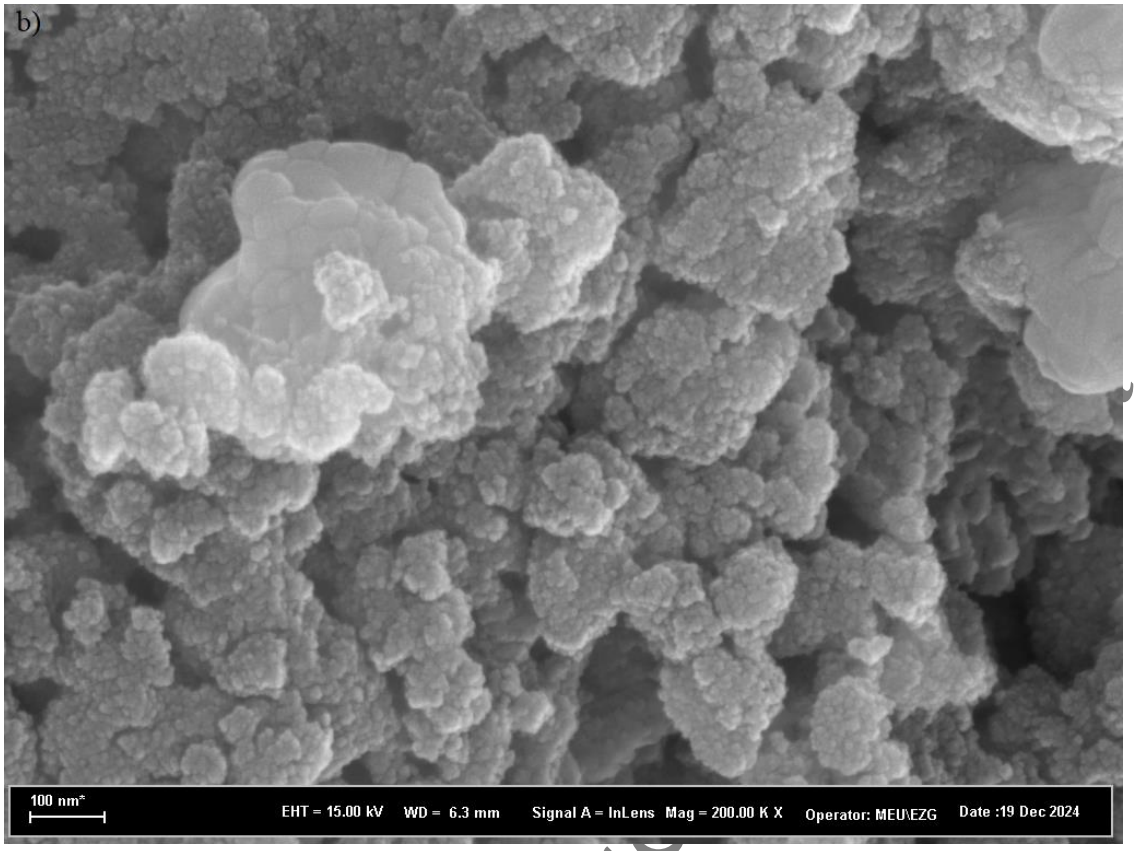
b)
100 nm*
EHT = 15.00 kV
WD = 6.3 mm
Signal A = InLens
Mag = 200.00 K X
Operator: MEU\EZG
Date :19 Dec 2024

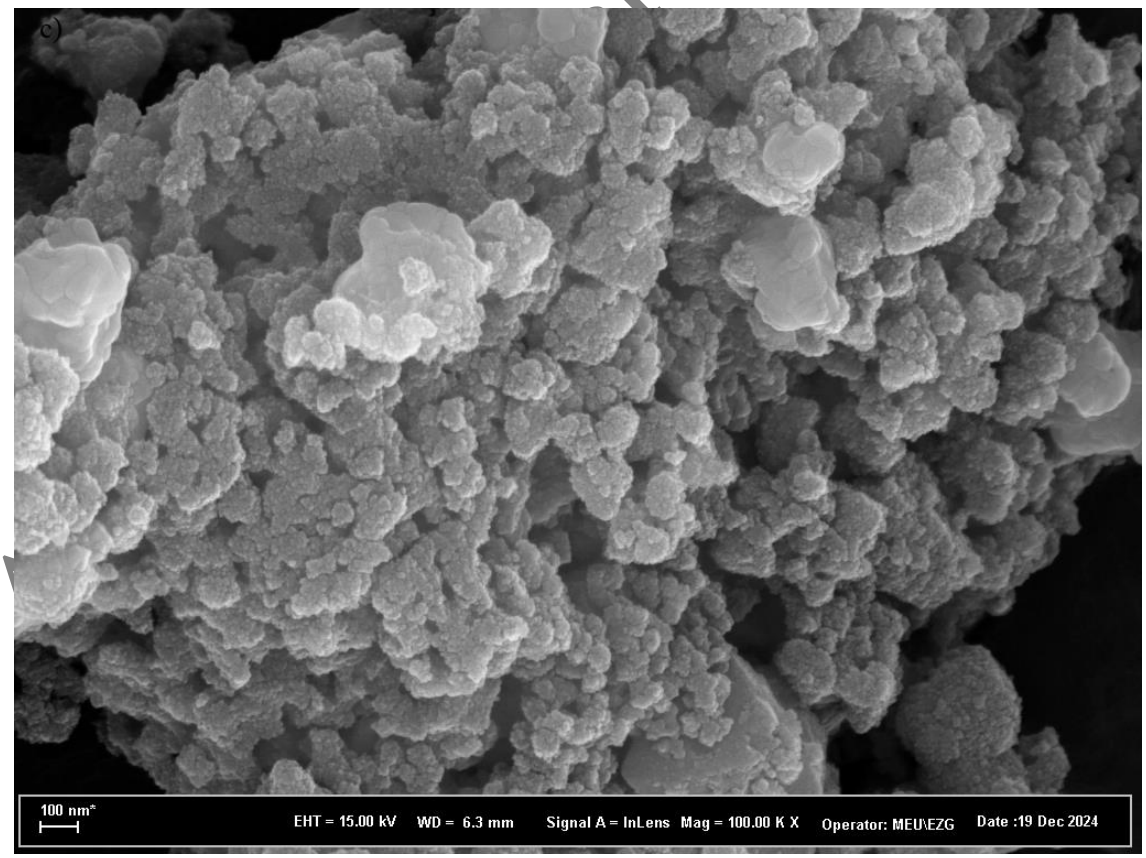
c)
100 nm*
EHT = 15.00 kV
WD = 6.3 mm
Signal A = InLens
Mag = 100.00 K X
Operator: MEU\EZG
Date :19 Dec 2024

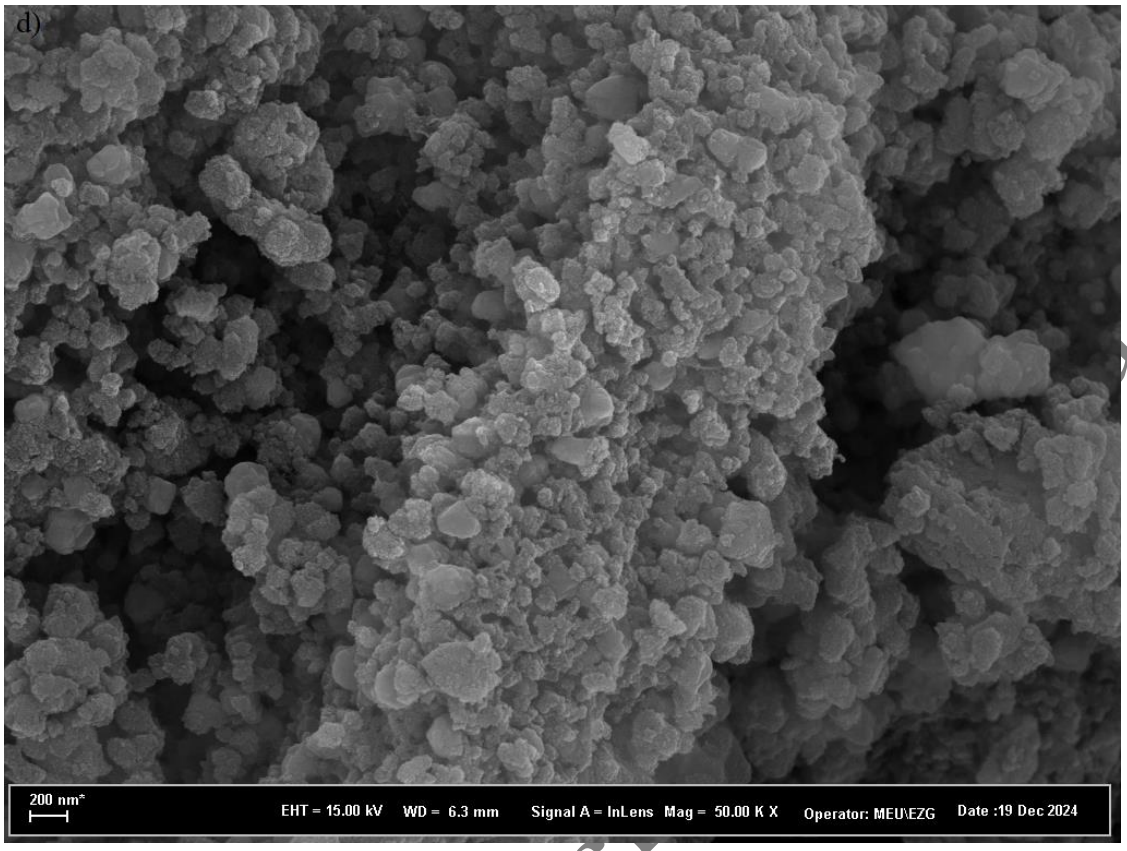
d)
200 nm*
EHT = 15.00 kV
WD = 6.3 mm
Signal A = InLens
Mag = 50.00 K X
Operator: MEU\EZG
Date :19 Dec 2024

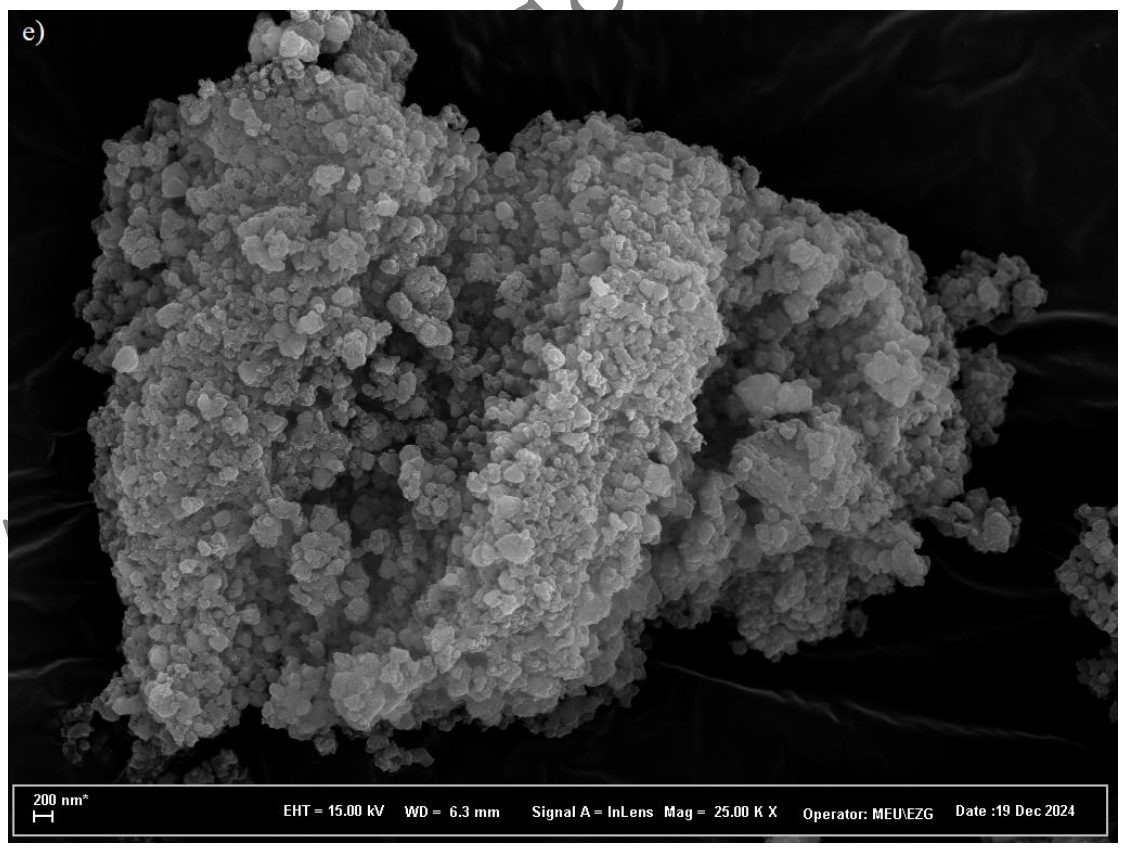
e)
200 nm*
EHT = 15.00 kV
WD = 6.3 mm
Signal A = InLens
Mag = 25.00 K X
Operator: MEU\EZG
Date :19 Dec 2024

Figure 2. SEM image of a KG CuTiZn NCs taken at magnifications of a) 400.00 K × , b)200.00 K ×, c) 100.00 K ×, d) 50.00 K ×, and e) 25.00 K ×

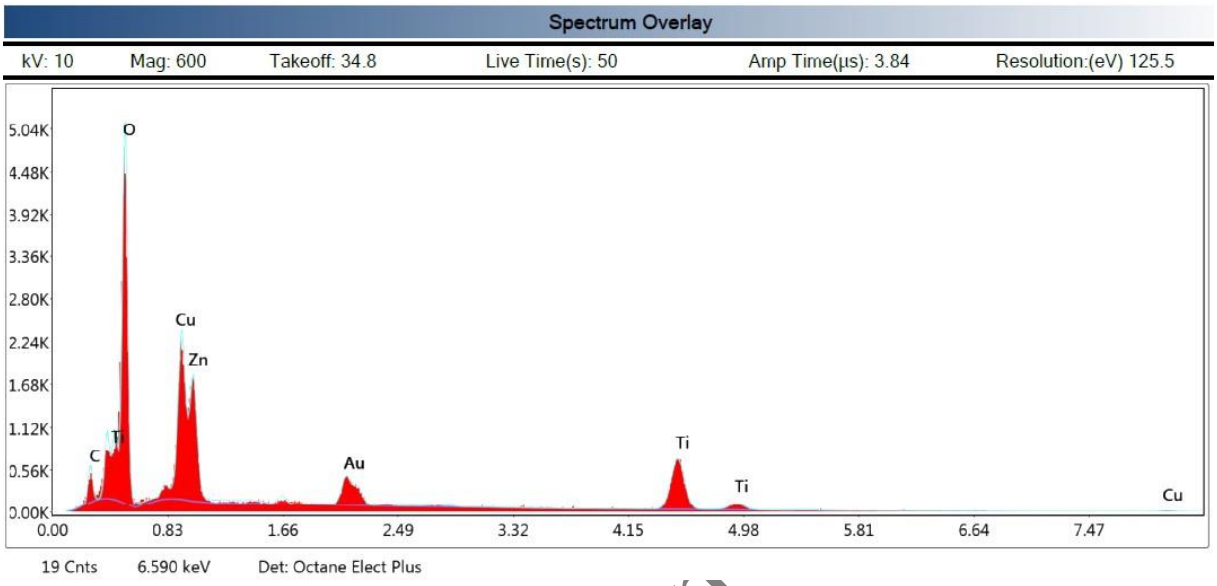

Figure 3. EDX spectra of the ternary CuTiZn nanocomposite.

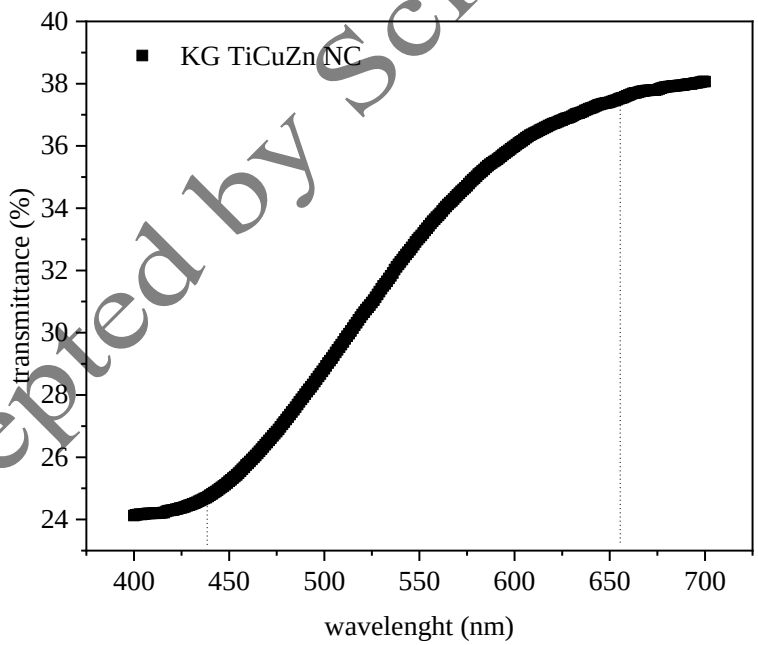

Figure 4. The transmittance graphs of CuTiZn NCs.

Accepted by Scien

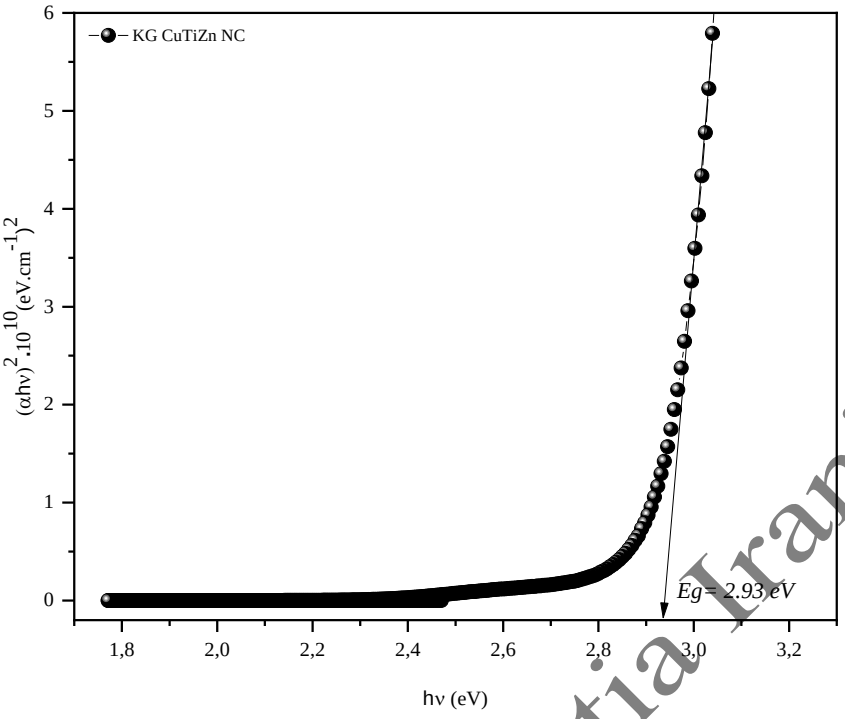

Figure 5. Plot of $(\alpha h\nu)^2$ and photon energy $(h\nu)$ for the CuTiZn NCs.

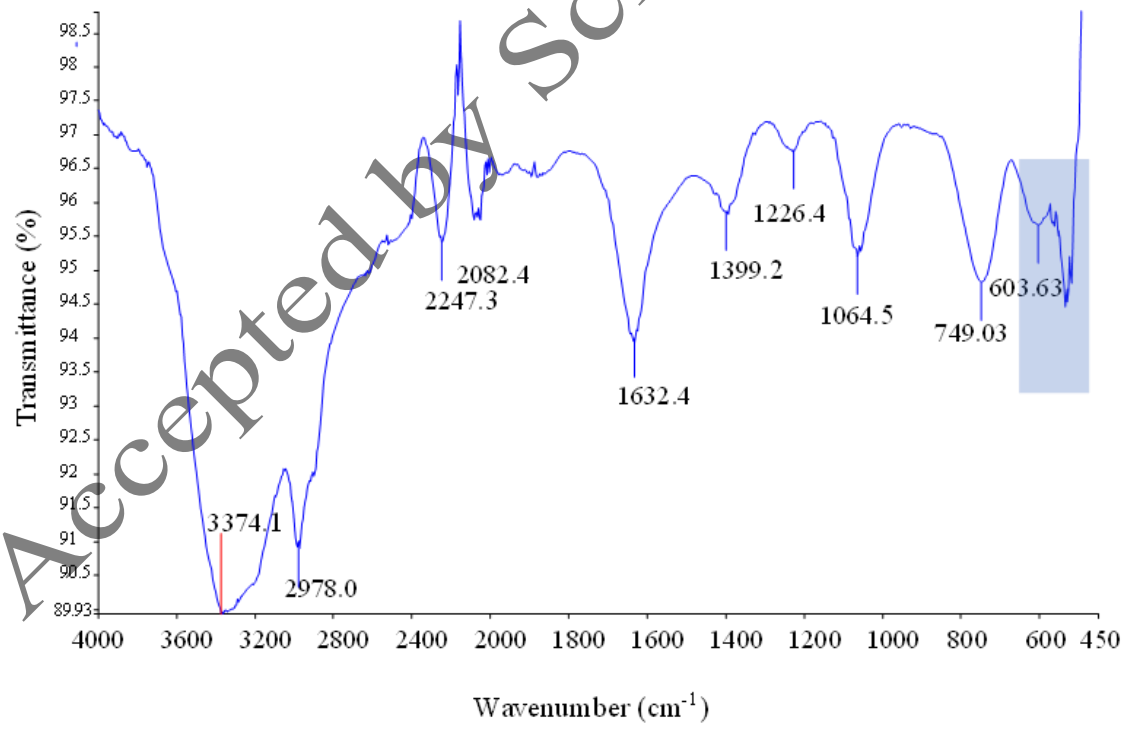

Figure 6. FTIR spectrum of CuTiZn NCs.

Accepted by Scientia Iranica

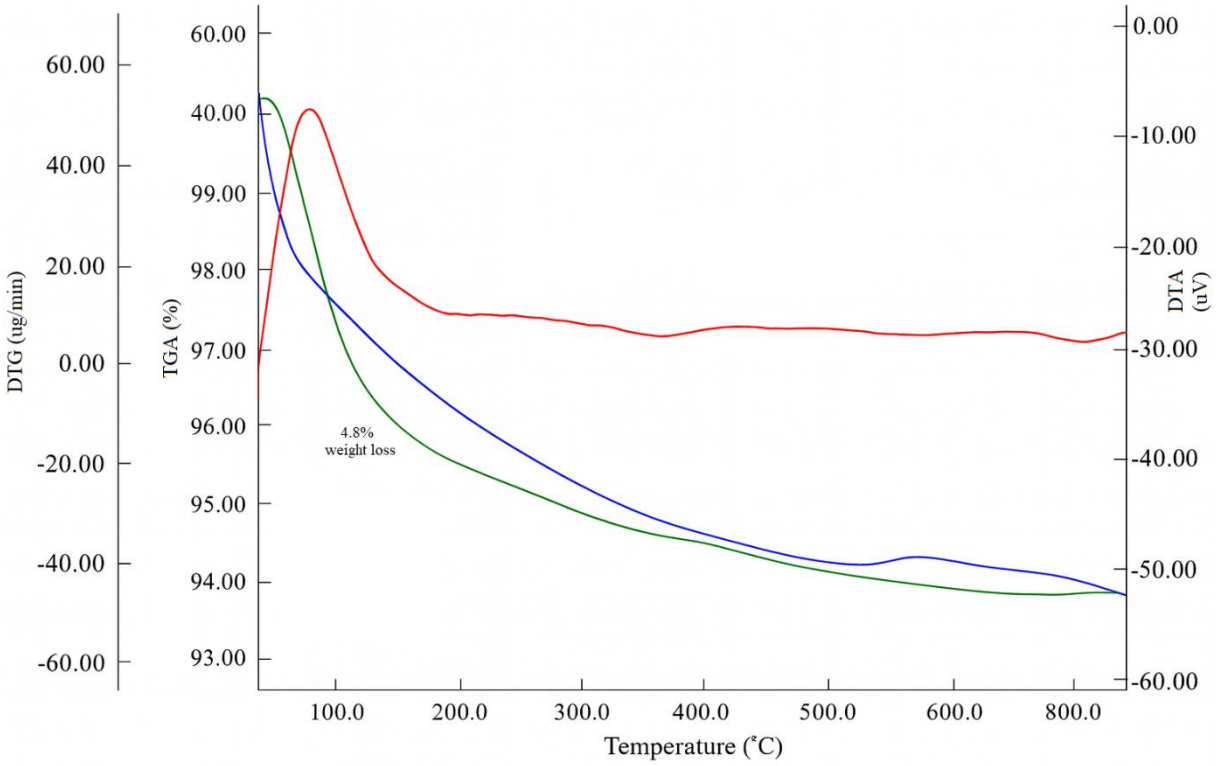

Figure 7. DTA-TGA spectrum of CuTiZn NCs.

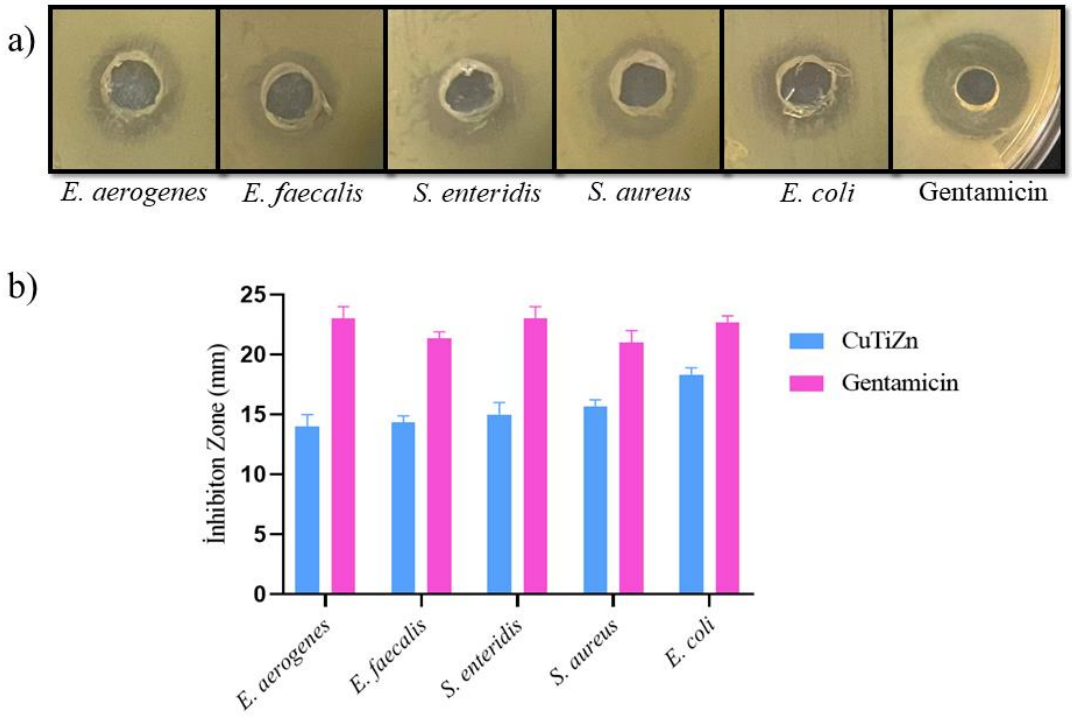

Figure 8. Antimicrobial activity of CuTiZn nanocomposite synthesized from *G. tournefortii* (kenger) gum. a) Representative image of inhibition zones for each pathogen, b) Quantitative comparison of inhibition zone diameters (mm) for each pathogen.

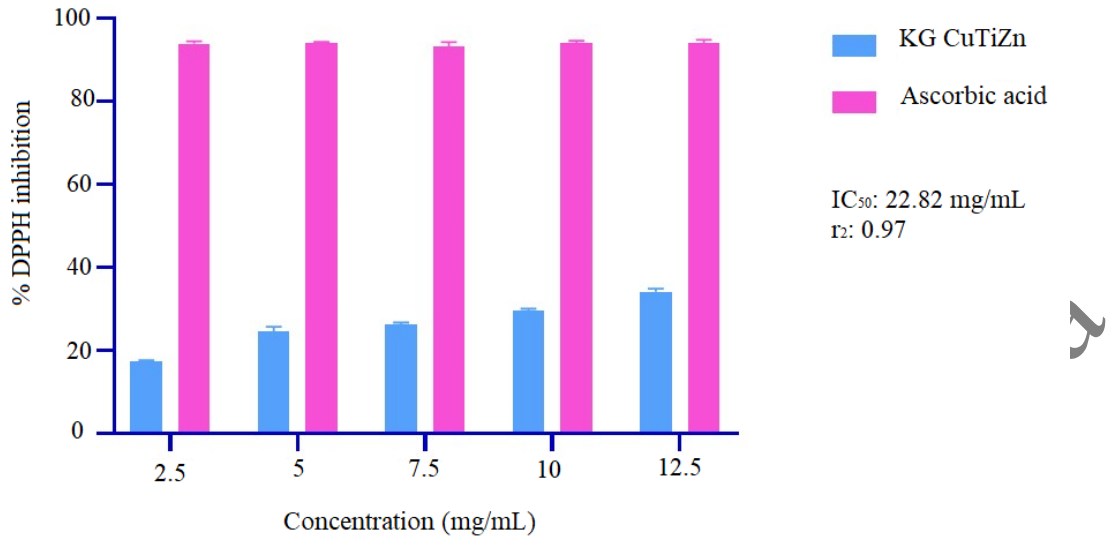

Figure 9. Antioxidant activity of the CuTiZn nanocomposite synthesized from *G. tournefortii* (kenger) gum, as evaluated via a DPPH radical scavenging assay.

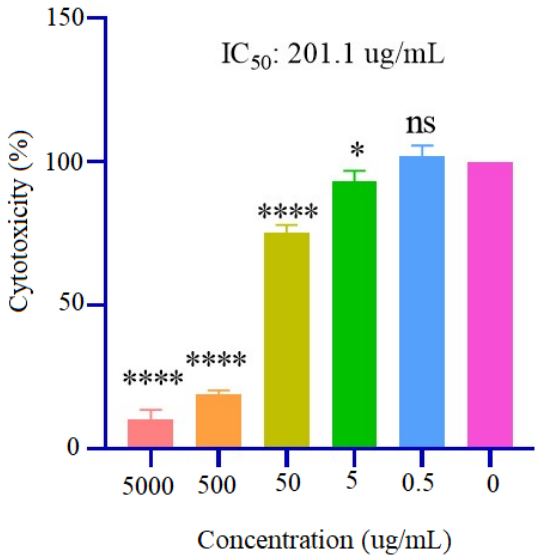

Figure 10. Cytotoxic activity of the CuTiZn nanocomposite synthesized with *G. tournefortii* (kenger) gum against MCF-7 breast cancer cells, as assessed via the MTT assay.

Table 1. XRD structural parameters of CuTiZn NCs.

Observed values		Standard values		(hkl)	Cristal size (nm)
2θ (°)	d (Å)	2θ (°)	d (Å)		
32.87	2.48	32.51	2.75	(110)	6.52
5.49	2.52	35.21	2.54	(311)	22.67
38.64	2.32	36.83	2.43	(222)	18.30
48.74	1.86	48.72	1.87	$(20\bar{2})$	20.77
61.51	1.50	62.11	1.49	$(11\bar{3})$	15.41
65.96	1.41	65.81	1.42	(022)	8.61

Table 2. EDX spectral parameters of the CuTiZn nanocomposite.

Map Sum Spectrum				
Element	Line Type	Weight %	Atomic %	Error %
C	K series	3.4	8.74	11.07
O	K series	29.62	57.16	8.88
Cu	L series	17.11	8.31	5.73
Zn	L series	14.91	7.04	7.18
Ti	K series	27.2	17.53	5.43
Au	M series	7.75	1.22	9.93
Total		100.00	100.00	100.00

Table 3. Antibacterial activity of CuTiZn NCs produced from Kenger gum on pathogenic strains.

Antimicrobial Zone Diameter (mm)					
	Gram negative			Gram positive	
	E. faecalis ATCC 29212	*S. aureus* ATCC 25923	*E. aerogenes* ATCC 13048	*S. enteridis* ATCC 13075	*E. coli* ATCC 25922
CuTiZn NCs	13.5±1	14.0±0.58	15±1	16.5±0.58	18±0.58
MIC (mg/mL)[a]					
	E. faecalis ATCC 29212	*S. aureus* ATCC 25923	*E. aerogenes* ATCC 13048	*S. enteridis* ATCC 13075	*E. coli* ATCC 25922
CuTiZn NCs	1.56	0.78	1.56	0.78	1.56

Accepted by Scientia Iranica

[a] MIC, minimum inhibitory concentrations;

Accepted by Scientia Iranica